JACS
JOURNAL OF THE AMERICAN CHEMICAL SOCIETY
Article
pubs.acs.org/JACS

Assembly of Peptides Derived from β-Sheet Regions of β-Amyloid

Nicholas L. Truex, Yilin Wang, and James S. Nowick*

Department of Chemistry, University of California, Irvine, Irvine, California 92697-2025, United States

Supporting Information

ABSTRACT: In Alzheimer's disease, aggregation of the β-amyloid peptide (Aβ) results in the formation of oligomers and fibrils that are associated with neurodegeneration. Aggregation of Aβ occurs through interactions between different regions of the peptide. This paper and the accompanying paper constitute a two-part investigation of two key regions of Aβ: the central region and the C-terminal region. These two regions promote aggregation and adopt β-sheet structure in the fibrils, and may also do so in the oligomers. In this paper, we study the assembly of macrocyclic β-sheet peptides that contain residues 17−23 (LVFFAED) from the central region and residues 30−36 (AIIGLMV) from the C-terminal region. These peptides assemble to form tetramers. Each tetramer consists of two hydrogen-bonded dimers that pack through hydrophobic interactions in a sandwich-like fashion. Incorporation of a single ^{15}N isotopic label into each peptide provides a spectroscopic probe with which to elucidate the β-sheet assembly and interaction: ^{1}H,^{15}N HSQC studies facilitate the identification of the monomers and tetramers; ^{15}N-edited NOESY studies corroborate the pairing of the dimers within the tetramers. In the following paper, *J. Am. Chem. Soc.* **2016**, DOI: 10.1021/jacs.6b06001, we will extend these studies to elucidate the coassembly of the peptides to form heterotetramers.

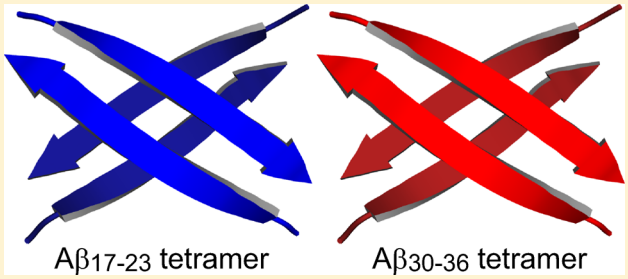

INTRODUCTION

Interaction among β-sheets is the two-edged sword in protein structure, imparting folding and stability but also driving misfolding and aggregation. While folding is typically associated with normal biological function, aggregation is associated with the pathology of Alzheimer's disease and other amyloid diseases, including Parkinson's disease and type II diabetes.[1] In Alzheimer's disease, the β-amyloid peptide (Aβ) aggregates to form oligomers and fibrils that characterize the disease pathology.[2]

Elucidation of the oligomers and fibrils is critical to understanding how Aβ aggregates and counteracting the harmful effects. The fibrils mark the thermodynamic end point of Aβ aggregation and accumulate as the disease progresses.[3] Several high-resolution structures have been reported of the Aβ fibrils, which typically adopt parallel β-sheet structure.[4,5] The oligomers are thought to be primarily responsible for neurodegeneration, causing synaptic dysfunction in neurons.[6] The oligomers are metastable and heterogeneous, and thus are difficult to study by high-resolution structural techniques.

Two key regions of Aβ favor β-sheet formation and promote aggregation: the central region and the C-terminal region.[7] The central region contains $Aβ_{17-21}$ (LVFFA). The two phenylalanine residues therein are especially important in nucleating and propagating the formation of Aβ aggregates.[8] The C-terminal region comprises residues AIIGLMVGGVV (for $Aβ_{1-40}$) or AIIGLMVGGVVIA (for $Aβ_{1-42}$). These successive hydrophobic residues also promote aggregation.[9]

The central and C-terminal regions of Aβ are thought to assemble in a different fashion in the fibrils than in the oligomers. In fibrils formed by $Aβ_{1-40}$, the two regions of the peptide can assemble to form layered parallel β-sheets connected by a U-shaped turn: one layer consists of the central region and the other consists of the C-terminal region.[4,5] Figure 1 illustrates a layered β-sheet structure formed by $Aβ_{1-40}$.[4b] These layered fibril structures can further assemble

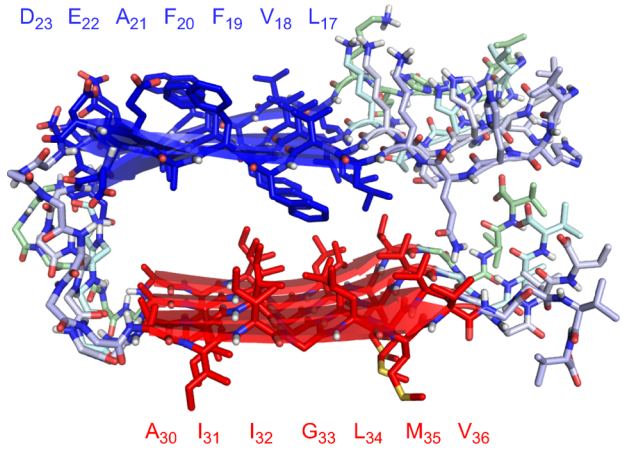

Figure 1. Layered β-sheet structure formed by $Aβ_{1-40}$ within β-amyloid fibrils (PDB ID: 2LMQ).

Received: June 10, 2016
Published: September 19, 2016

DOI: 10.1021/jacs.6b06000
J. Am. Chem. Soc. 2016, 138, 13882−13890

in twos and threes to form fibrils that exhibit two-fold or three-fold symmetry. In the oligomers, the central and C-terminal regions are thought to coassemble in an antiparallel fashion to form β-hairpins, which assemble to form the oligomers.[10] These regions may also promote the assembly of Aβ to form higher-order oligomers.

In 2012, our research group introduced macrocyclic β-sheet peptides **1** as a model system to investigate the assembly of amyloidogenic peptides and proteins (Figure 2).[11] Peptides **1**

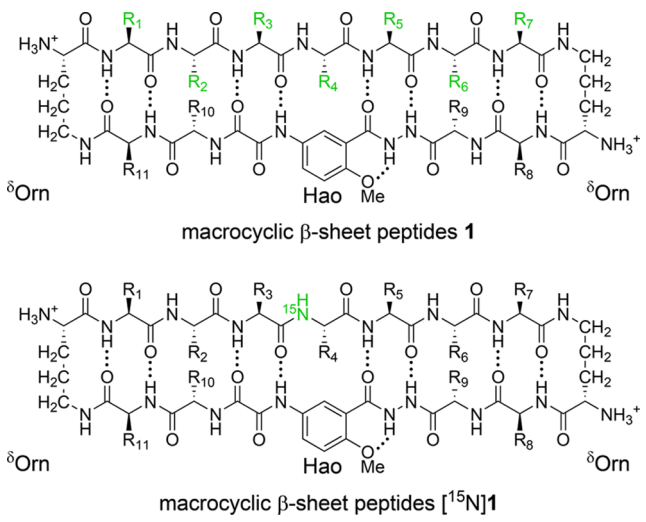

Figure 2. Macrocyclic β-sheet peptides **1**, illustrating the heptapeptide strand (upper strand), the template strand (lower strand), and the two $^{\delta}$Orn turn units. Macrocyclic β-sheet peptides [^{15}N]**1**, illustrating the ^{15}N isotopic label at the R_4 position.

consist of a heptapeptide strand (R_{1-7}), a template strand, and two turn units. The heptapeptide strand displays amyloidogenic peptide sequences. The template strand contains the unnatural amino acid Hao and four additional residues (R_{8-11}) that help promote β-sheet structure. Hao is a tripeptide mimic that templates β-sheet hydrogen bonding and blocks uncontrolled aggregation.[12] The δ-linked ornithine ($^{\delta}$Orn) turn units on each side connect the two strands and allow β-sheet folding.[13] Our research group incorporated hydrophilic residues at positions R_8 and/or R_{11} to minimize oligomerization.

In this two-part investigation, we incorporated residues from the central and C-terminal regions of Aβ into peptides **1** to ask whether these regions prefer to coassemble or to segregate.[14] To promote the formation of well-defined oligomers, we incorporated hydrophobic residues into positions R_8 and R_{11}. The first part—the current paper—determines how the two peptides assemble in aqueous solution. The second part—the accompanying paper—determines whether the two peptides exhibit a special preference to coassemble when mixed.[15] This question is important because the two regions generally segregate in the fibrils but coassemble in the oligomers.

To facilitate these studies, we incorporated ^{15}N isotopic labels into peptides **1**. Peptides [^{15}N]**1** contain a single ^{15}N isotopic label at the R_4 position in the center of the heptapeptide strand (Figure 2). These peptides are readily prepared from commercially available ^{15}N-labeled amino acids using solid-phase peptide synthesis. The ^{15}N isotopic label provides a simple and effective spectroscopic probe to monitor assembly and coassembly by ^{1}H,^{15}N NMR spectroscopy.

RESULTS AND DISCUSSION

Design of Peptides Derived from the Central and C-Terminal Regions of Aβ. We incorporated residues LVFFAED (Aβ_{17-23}) and AIIGLMV (Aβ_{30-36}) into peptides **1**, to give peptides **1a** and **1b**. We designed the peptides with a distinct hydrophobic surface to promote assembly by incorporating isoleucine residues at positions R_8 and R_{11} of the template strand. We also designed the peptides with a hydrophilic surface to promote solubility and prevent uncontrolled aggregation by incorporating lysine residues at positions R_9 and R_{10} of the template strand.

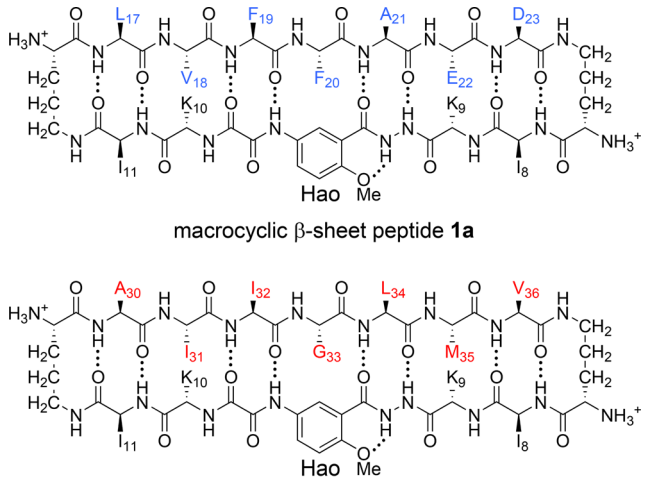

^{1}H NMR studies show that peptides **1a** and **1b** assemble to form sandwich-like tetramers in aqueous solution.[16] The tetramers consist of two β-sheet dimers that stack like slices of bread. The dimers are stabilized by hydrogen-bonding interactions between the amide backbones of the heptapeptide strands; the tetramers are stabilized by hydrophobic interactions between the hydrophobic surfaces of the dimers. The following subsections describe the elucidation of the tetramers by NMR spectroscopy.

DOSY Shows That Peptides 1a and 1b Form Tetramers. Our laboratory has previously used DOSY NMR studies and corroboratory analytical ultracentrifugation (AUC) experiments to establish that related macrocyclic β-sheet peptides form tetramers.[17] DOSY NMR studies of peptides **1a** and **1b** show that these macrocyclic β-sheets also form tetramers (Table 1). The DOSY spectrum of peptide **1a** at 0.15 mM shows two sets of resonances: one set from the monomer, with a diffusion coefficient of 20.4×10^{-11} m^2/s; the other set from the tetramer, with a diffusion coefficient of 12.6×10^{-11} m^2/s. At 8.0 mM, the spectrum shows only the latter set of resonances with a diffusion coefficient of 11.8×10^{-11} m^2/s.

Table 1. Diffusion Coefficients (D) of Peptides 1a and 1b in D_2O at 298 K

	$MW_{monomer}$[a] (Da)	$MW_{tetramer}$[a] (Da)	conc. (mM)	D ($\times 10^{-11}$ m^2/s)	oligomer state
1a	1767	7068	0.15	20.4 ± 1.7	monomer
			0.15	12.6 ± 1.6	tetramer
			8.0	11.8 ± 1.0	tetramer
1b	1643	6572	1.0	19.4 ± 1.7	monomer
			16.0	11.9 ± 1.1	tetramer

[a]Molecular weight calculated for the neutral (uncharged) peptide.

DOI: 10.1021/jacs.6b06000
J. Am. Chem. Soc. 2016, 138, 13882−13890

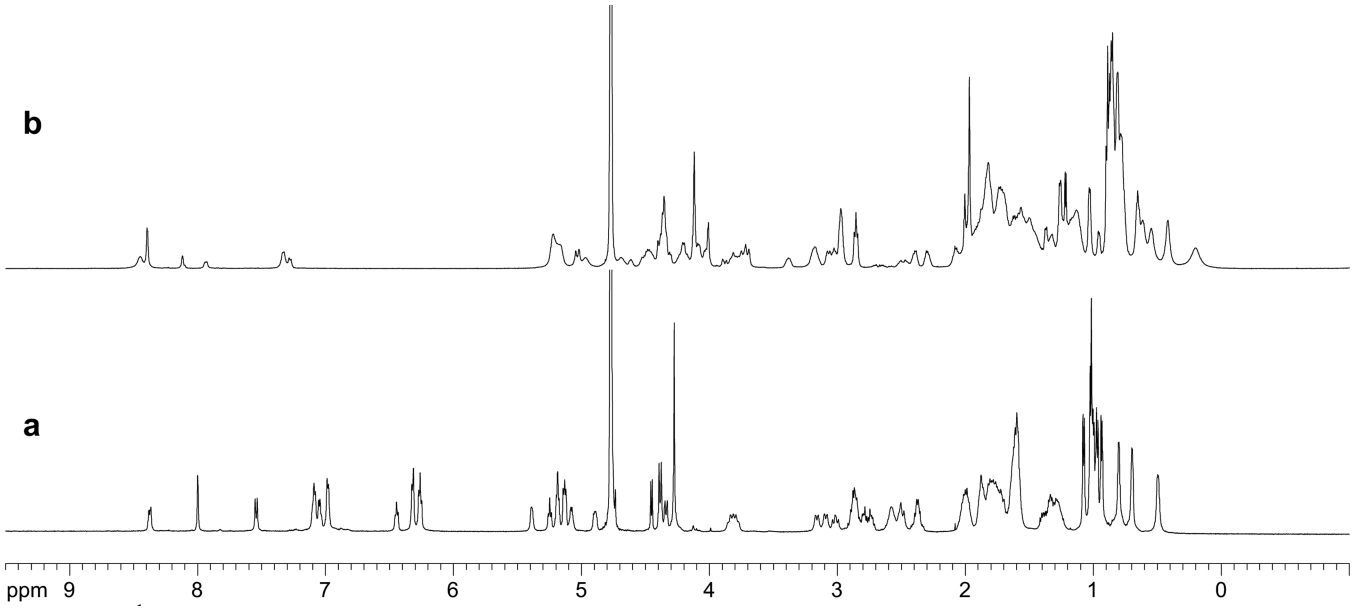

Figure 3. ^{1}H NMR spectra of (a) peptide **1a** and (b) peptide **1b** at 8.0 mM in D_2O at 600 MHz and 298 K.

The DOSY spectrum of peptide **1b** at 1.0 mM shows resonances from the monomer, with a diffusion coefficient 19.4×10^{-11} m^2/s, and the spectrum at 16.0 mM shows resonances from the tetramer, with a diffusion coefficient of 11.9×10^{-11} m^2/s.

The ratio of diffusion coefficients of a tetramer and monomer is typically 0.6.[18] DOSY studies show that the oligomers of peptides **1a** and **1b** have diffusion coefficients of about 12×10^{-11} m^2/s and the monomers have diffusion coefficients of about 20×10^{-11} m^2/s. The ratio of the diffusion coefficients (0.6) is consistent with a tetramer.[19]

Elucidation of the Peptide 1a Tetramer. Peptide **1a** forms a tetramer that consists of two β-sheet dimers. The ^{1}H NMR spectrum of peptide **1a** at 8 mM in D_2O at 298 K shows one predominant set of resonances (Figure 3a).[20] These resonances are associated with the tetramer. The resonances are disperse and exhibit distinct spectral features that reflect well-defined β-sheet structure: Seven of the 11 α-protons appear downfield of 5 ppm. The methyl proton resonance of A_{21} appears at 0.5 ppm. The aromatic proton resonances of F_{19} appear upfield of 7 ppm (6.3 to 6.5 ppm). The ^{1}H NMR spectrum of peptide **1a** at 0.15 mM in D_2O at 298 K shows resonances associated with both the monomer and the tetramer (Figure S1). The resonances of the monomer lack the distinct spectral features of the tetramer.

The magnetic anisotropy of the diastereotopic δ-proton resonances of the $^{\delta}$Orn turn units reflects β-sheet folding in peptides **1** and related macrocyclic β-sheets.[11a,13] In a well-folded macrocyclic β-sheet, the diasterotopic *pro-S* δ-protons appear about 0.6 ppm downfield of the *pro-R* δ-protons. In the tetramer of peptide **1a**, the *pro-S* δ-protons appear 0.63 and 0.74 ppm downfield of the *pro-R* δ-protons. In the monomer, the *pro-S* δ-protons of peptide **1a** appear 0.30 and 0.39 ppm downfield of the *pro-R* δ-protons. The magnetic anisotropies of these proton resonances indicate that the monomer is moderately folded, while the tetramer is well folded.

The NOESY spectrum of peptide **1a** shows strong NOEs associated with the β-sheet folding and assembly of the tetramer. The spectrum shows a network of five strong NOEs associated with β-sheet folding: between the α-protons of V_{18} and K_{10}, the α-protons of E_{22} and K_9, the α-proton of F_{20} and the proton at the 6-position of the unnatural amino acid Hao ($HaoH_6$), and the α- and δ-protons of the $^{\delta}$Orn turn units (Figure S2). The spectrum shows two additional NOEs associated with β-sheet dimerization, between the α-protons of L_{17} and D_{23} and between the α-protons of F_{19} and A_{21} (Figure S2a). Figure 4 illustrates the dimer of peptide **1a** consistent with these NOEs.

The NOESY spectrum shows additional NOEs associated with the stacking of two dimers to form a sandwich-like tetramer. The spectrum shows a pattern of NOEs between the methoxy protons of Hao (Hao_{OMe}) and the side-chain protons of I_{11}, and additional NOEs between the protons at the 3- and 4-positions of Hao ($HaoH_3$ and $HaoH_4$) and the δ-methyl protons of I_{11} (Figure S3). Figure 4 illustrates the stacking of the two dimers of peptide **1a** consistent with these interlayer NOEs.

Elucidation of the Peptide 1b Tetramer. Peptide **1b** forms a similar tetramer, which also consists of two β-sheet dimers. The tetramer is less stable than that formed by peptide **1a** and is in equilibrium with substantial amounts of monomer at millimolar concentrations (Figure S4). The ^{1}H NMR spectrum of peptide **1b** at 8.0 mM in D_2O at 298 K shows two sets of resonances. These resonances appear in a 3:2 ratio of intensities, with the predominant set associated with the tetramer and the smaller set associated with the monomer (Figure 3b). The resonances are broadened, reflecting chemical exchange between the tetramer and the monomer on a ca. hundred-millisecond time scale. The resonances associated with the tetramer exhibit several distinct spectral features that reflect well-defined β-sheet structure: Five of the 11 α-proton resonances appear downfield of 5 ppm. The methyl proton resonances of L_{34} are shifted upfield of 0.5 ppm (0.38 and 0.12 ppm). The *pro-S* δ-proton resonances of the $^{\delta}$Orn turn units appear 0.65 and 0.69 ppm downfield of the *pro-R* δ-proton resonances.

The monomer of peptide **1b** lacks these distinct spectral features. The *pro-S* δ-proton resonances of the $^{\delta}$Orn turn units

DOI: 10.1021/jacs.6b06000
J. Am. Chem. Soc. 2016, 138, 13882−13890

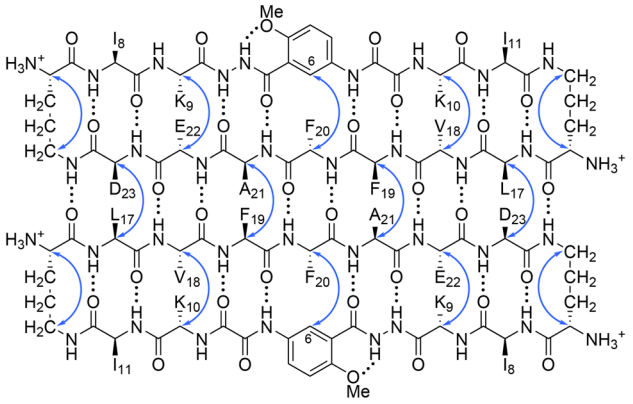

dimer of peptide **1a**

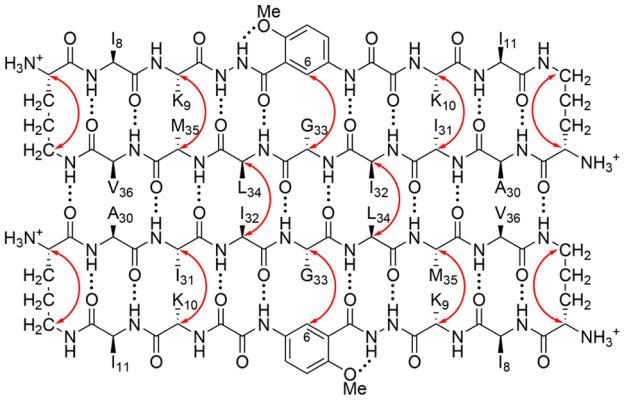

dimer of peptide **1b**

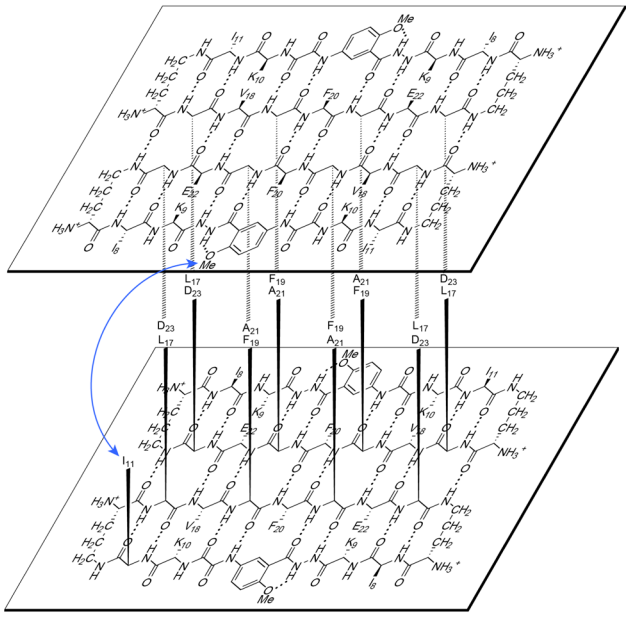

tetramer of peptide **1a**

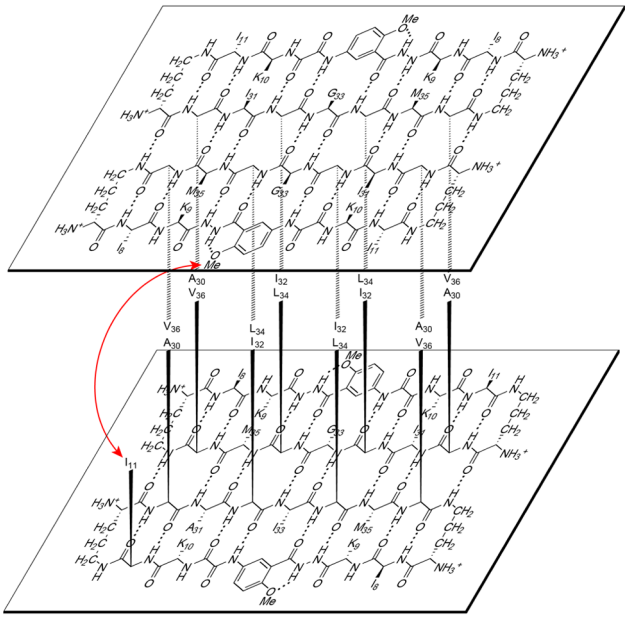

tetramer of peptide **1b**

Figure 4. Dimer and tetramer of peptide **1a**. Hydrogen-bonded dimer subunit (upper). Blue arrows illustrate intramolecular and intermolecular NOEs observed in the NOESY spectrum. Sandwich-like tetramer consisting of two hydrogen-bonded dimers (lower). The blue arrow illustrates the interlayer NOEs observed in the NOESY spectrum. The tetramer exhibits four-fold symmetry and four I_{11}–Hao_{OMe} interactions, even though only one arrow is shown.

Figure 5. Dimer and tetramer of peptide **1b**. Hydrogen-bonded dimer subunit (upper). Red arrows illustrate intramolecular and intermolecular NOEs observed in the NOESY spectrum. Sandwich-like tetramer consisting of two hydrogen-bonded dimers (lower). The red arrow illustrates the interlayer NOEs observed in the NOESY spectrum. The tetramer exhibits four-fold symmetry and four I_{11}–Hao_{OMe} interactions, even though only one arrow is shown.

appear 0.16 and 0.19 ppm downfield of the *pro-R* δ-proton resonances. The magnetic anisotropies of these proton resonances indicate that the monomer is poorly folded. In contrast to peptide **1a**, the monomer of peptide **1b** predominates at low millimolar concentrations. At concentrations below 1 mM, the spectrum shows almost exclusively the monomer and virtually no tetramer.

The NOESY spectrum of peptide **1b** shows strong NOEs associated with β-sheet folding and weaker NOEs associated with β-sheet assembly. The spectrum shows a network of five strong NOEs associated with β-sheet folding: between the α-protons of I_{31} and K_{10}, the α-protons of M_{35} and K_9, the *pro-R* α-proton of G_{33} and the $HaoH_6$ proton, and the α- and δ-protons of the $^{\delta}$Orn turn units (Figure S5). The spectrum shows an additional NOE associated with β-sheet dimerization, between the α-protons of I_{32} and L_{34} (Figure S5a). The spectrum does not show a well-defined NOE crosspeak between the α-protons of A_{30} and V_{36}. The absence of a well-defined crosspeak may reflect broadening of the resonances through chemical exchange with the monomer and overlap with an exchange crosspeak, or it may reflect a lack of close contact between the two protons. Figure 5 illustrates the β-sheet folding and dimerization of peptide **1b** consistent with these NOEs.

The NOESY spectrum shows additional NOEs associated with the stacking of two dimers to form a sandwich-like tetramer. Like peptide **1a**, peptide **1b** exhibits a pattern of NOEs between the Hao protons and the I_{11} side-chain protons, and an additional NOE between $HaoH_3$ and the δ-methyl protons of I_{11} (Figure S6). Figure 5 illustrates the stacking of the two dimers of peptide **1b** consistent with these interlayer NOEs.

DOI: 10.1021/jacs.6b06000
J. Am. Chem. Soc. 2016, 138, 13882–13890

^{1}H,^{15}N HSQC Studies of the Tetramers Formed by Peptides [^{15}N]1a and [^{15}N]1b. We studied ^{15}N-labeled homologues of peptides **1a** and **1b** by ^{1}H,^{15}N HSQC to identify and quantify the tetramers. ^{1}H,^{15}N HSQC is a mainstay in NMR spectroscopy of proteins, but is also useful for peptides. ^{15}N-Isotopic labeling and the dispersion provided by the f_1 (^{15}N) dimension resolves mixtures of peptides far better than is possible by homonuclear techniques.

We prepared peptides [^{15}N]**1a** and [^{15}N]**1b**, which each contain a single ^{15}N-labeled amino acid in the center of the heptapeptide strand. Peptide [^{15}N]**1a** contains an ^{15}N-labeled phenylalanine; peptide [^{15}N]**1b** contains an ^{15}N-labeled glycine. The ^{15}N isotopic label provides a spectroscopic probe for each species containing the ^{15}N-labeled peptide.

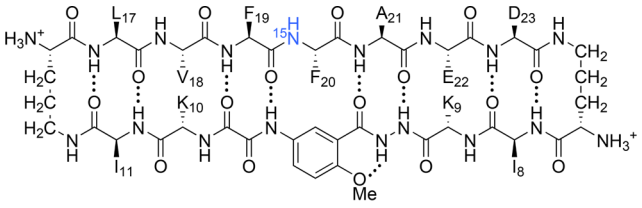

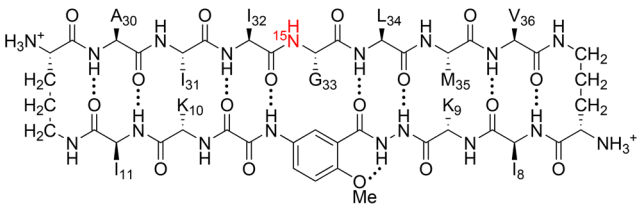

The ^{1}H,^{15}N HSQC spectrum of peptide [^{15}N]**1a** in 9:1 H_2O/D_2O at 8.0 mM and 293 K shows two crosspeaks; the ^{1}H,^{15}N HSQC spectrum of peptide [^{15}N]**1b** also shows two crosspeaks (Figure 6). The spectrum of peptide [^{15}N]**1a** shows a weak crosspeak associated with the monomer and a strong crosspeak associated with the tetramer; these crosspeaks are designated 1 and 2, respectively. The spectrum of peptide [^{15}N]**1b** shows crosspeaks of comparable intensities associated with the monomer and tetramer; these crosspeaks are designated 3 and 4, respectively. Table 2 summarizes the chemical shifts of these crosspeaks.

In the accompanying paper, we combine ^{15}N-labeling and ^{1}H,^{15}N NMR spectroscopy to identify and characterize the seven different species that form upon mixing peptides [^{15}N]**1a** and [^{15}N]**1b**.[15]

^{15}N-Edited NOESY. We used peptides [^{15}N]**1a** and [^{15}N]**1b** to corroborate the pairing of the dimers within the tetramers. We recorded ^{1}H,^{15}N NOESY-HSQC spectra with typical NOESY parameters in both ^{1}H dimensions (f_1 and f_3), but with only one increment in the ^{15}N dimension (f_2). The result is an ^{15}N-edited NOESY spectrum that shows only NOEs involving the ^{15}NH protons and requires no more time than a regular NOESY spectrum.

The NH protons of an antiparallel β-sheet typically give a pattern of four key NOEs associated with β-sheet folding and interstrand interaction. Two of the NOEs reflect β-sheet folding: a weaker intraresidue NOE to the α-proton and a stronger interresidue NOE to the α-proton of the adjacent residue. Figure 7 illustrates these close contacts and shows typical distances (3.0 and 2.2 Å, respectively). Two of the

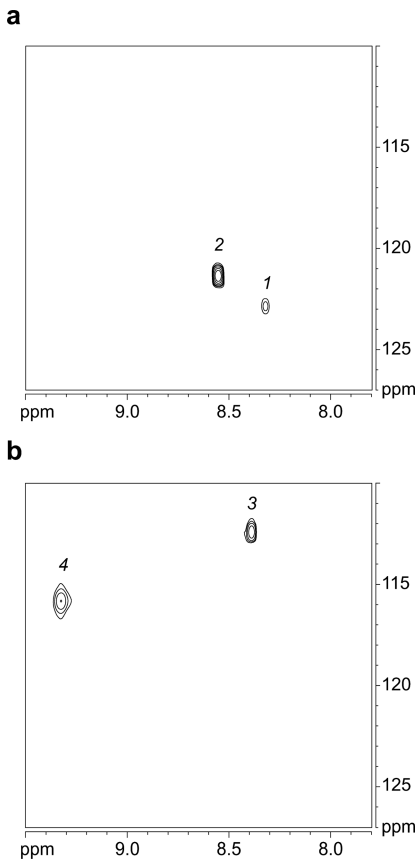

Figure 6. ^{1}H,^{15}N HSQC spectra of (a) peptide [^{15}N]**1a** and (b) peptide [^{15}N]**1b** at 8.0 mM in 9:1 H_2O/D_2O at 600 MHz and 293 K.

Table 2. Chemical Shifts of Peptides [^{15}N]1a and [^{15}N]1b

	δ F_{20}		δ G_{33}		
crosspeak	^{1}H	^{15}N	^{1}H	^{15}N	species
1	8.32	122.3			A monomer
2	8.56	121.3			A_4 tetramer
3			8.39	112.5	B monomer
4			9.33	115.8	B_4 tetramer

[a] ^{1}H,^{15}N HSQC spectra were recorded at 8.0 mM in 9:1 H_2O/D_2O at 293 K.

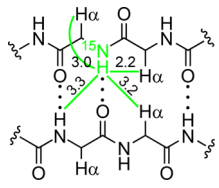

Figure 7. Four close contacts involving NH protons and Hα protons in antiparallel β-sheets. Typical distances are shown in angstroms.

NOEs reflect interstrand interaction: an NOE to the α-proton diagonally across in the non-hydrogen-bonded pair, and another NOE to the NH proton diagonally across in the hydrogen-bonded pair. Figure 7 also illustrates these close contacts and shows typical distances (3.2 and 3.3 Å, respectively). The magnitude of the interresidue NOE should be much stronger than the magnitude of the interstrand NOEs, because the NOE intensities decrease with distance to the inverse sixth power.

DOI: 10.1021/jacs.6b06000
J. Am. Chem. Soc. 2016, 138, 13882−13890

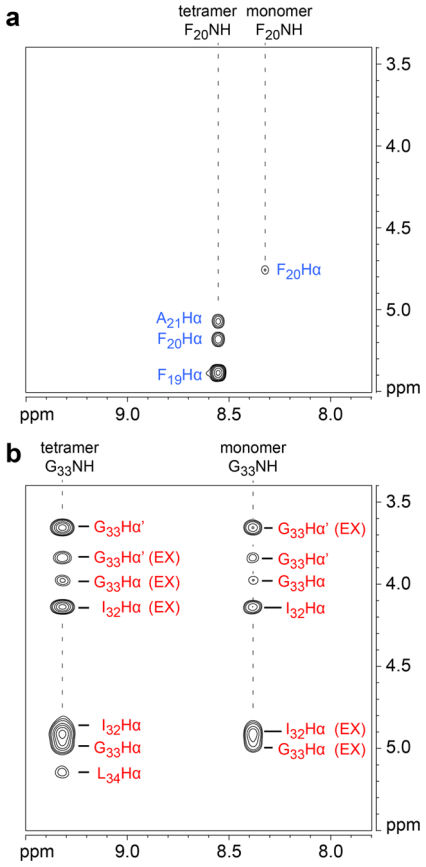

Figure 8. ^{15}N-Edited NOESY spectra of (a) peptide [^{15}N]**1a** and (b) peptide [^{15}N]**1b** at 8.0 mM in 9:1 H_2O/D_2O at 600 MHz and 293 K. The $G_{33}H\alpha$ corresponds to the *pro-R* α-proton and the $G_{33}H\alpha'$ corresponds to the *pro-S* α-proton. Crosspeaks associated with chemical exchange between the monomer and tetramer are labeled EX.[20]

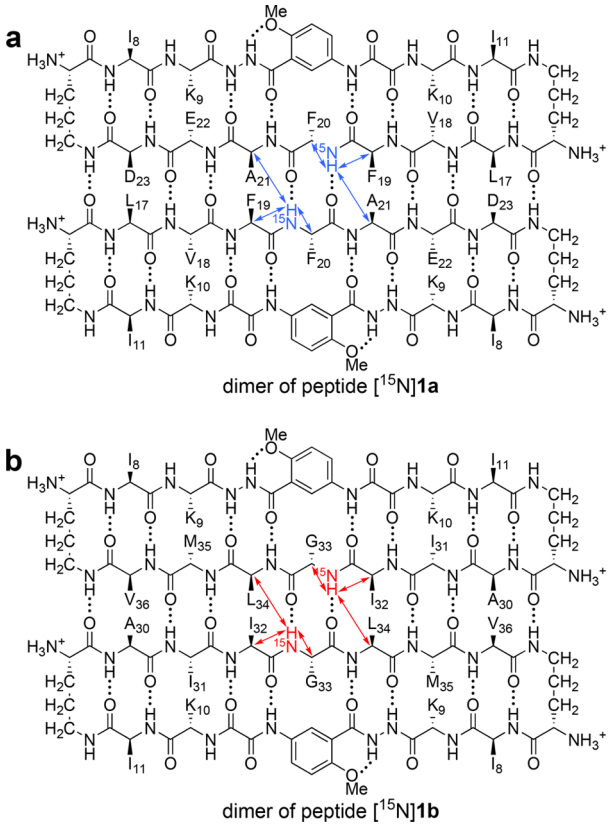

Figure 9. NOEs involving the ^{15}NH protons between the dimers of peptides [^{15}N]**1a** and [^{15}N]**1b** within the respective tetramers. Blue and red arrows illustrate observed NOEs.

The ^{15}N-edited NOESY spectrum of peptide [^{15}N]**1a** shows two sets of NOEs: one set is associated with the F_{20}NH proton from the monomer; the other set is associated with the F_{20}NH proton from the tetramer (Figure 8a). The monomer F_{20}NH proton gives only an intraresidue NOE to the $F_{20}H\alpha$ proton. The tetramer F_{20}NH proton gives two NOEs associated with β-sheet folding: a stronger interresidue NOE to the $F_{19}H\alpha$ proton and an intraresidue NOE to the $F_{20}H\alpha$ proton. The tetramer F_{20}NH proton also gives an intermolecular NOE associated with interstrand interaction to the $A_{21}H\alpha$ proton diagonally across the peptide dimer. This NOE is significant, because it reflects the dimer within the tetramer (Figure 9a). The tetramer F_{20}NH proton can not give an intermolecular NOE to the F_{20}NH proton diagonally across the peptide dimer, because the tetramer is symmetrical (Figure S7). Figure 9 summarizes the observed NOEs involving the ^{15}NH protons between the dimers within the tetramer of peptide [^{15}N]**1a**.

The ^{15}N-edited NOESY spectrum of peptide [^{15}N]**1b** also shows two sets of NOEs: one set is associated with the G_{33}NH proton from the monomer; the other set is associated with the G_{33}NH proton from the tetramer (Figure 8b). The monomer G_{33}NH proton gives a pattern of NOEs associated with β-sheet folding: two intraresidue NOEs to the diastereotopic $G_{33}H\alpha$ and $G_{33}H\alpha'$ protons and one interresidue NOE to the $I_{32}H\alpha$ proton. The tetramer G_{33}NH proton also gives a pattern of NOEs associated with β-sheet folding: two intraresidue NOEs to the $G_{33}H\alpha$ and $G_{33}H\alpha'$ protons and one interresidue NOE to the $I_{32}H\alpha$ proton. The tetramer G_{33}NH proton also gives an intermolecular NOE associated with interstrand interaction to the $L_{34}H\alpha$ proton diagonally across the peptide dimer. This NOE is significant, because it reflects the dimer within the tetramer. The tetramer G_{33}NH proton can not give an intermolecular NOE to the G_{33}NH proton diagonally across the peptide dimer, because the tetramer is symmetrical (Figure S8). Figure 9 summarizes the observed NOEs involving the ^{15}NH protons between the dimers within the tetramer of peptide [^{15}N]**1b**.

Molecular Models of the Tetramers. We constructed energy-minimized models consistent with the observed NOEs to help understand the structures of the tetramers of peptides **1a** and **1b**. We began with the X-ray crystallographic coordinates of a tetramer formed by a homologous macrocyclic β-sheet peptide (PDB ID: 3T4G).[11a] We mutated the side chains to the residues of peptides **1a** and **1b**. We modified the alignment of the β-sheet dimers and oriented the dimers to reflect the observed NOEs. We then generated the minimum-energy models (local minima) of the tetramers. These models help illustrate the structures formed by the peptides derived from the central and C-terminal regions of Aβ. Figures 10 and 11 illustrate these models.

The energy-minimized model of the peptide **1a** tetramer consists of a β-sandwich of two four-stranded β-sheets that laminate together and form a hydrophobic core (Figure 10). The β-sheets exhibit a distinct twist that imparts a saddle shape. The side chains of L_{17}, F_{19}, and A_{21} form a hydrophobic surface that packs in the hydrophobic core, while the side chains of E_{22}

DOI: 10.1021/jacs.6b06000
J. Am. Chem. Soc. 2016, 138, 13882−13890

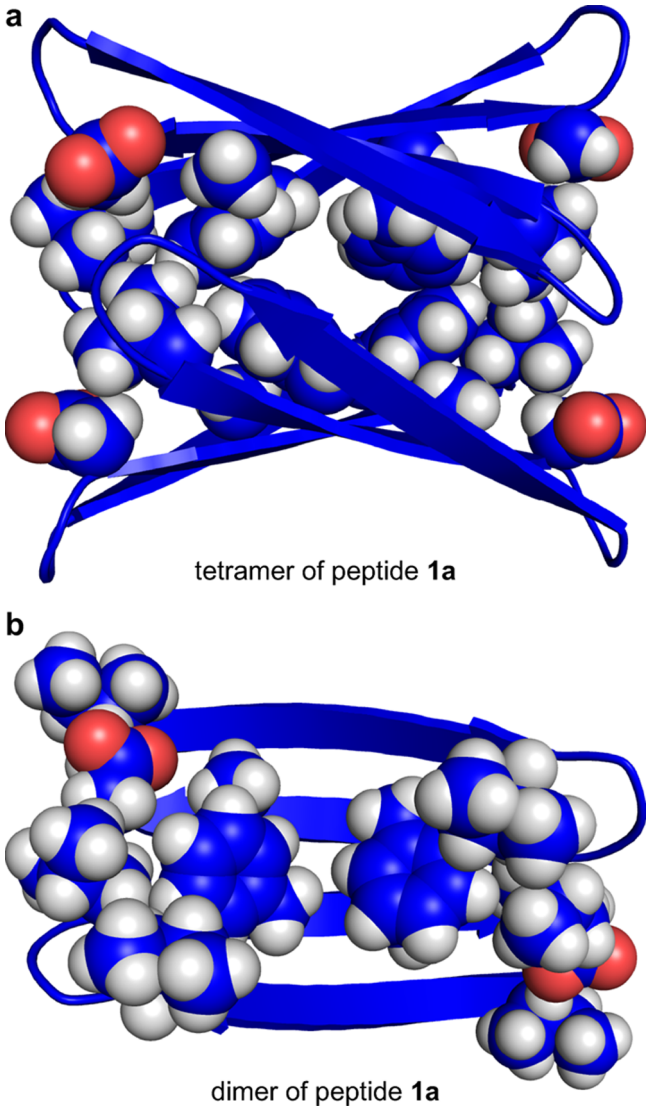

Figure 10. Molecular model of the tetramer formed by peptide **1a**. (a) The tetramer with the side chains of L_{17}, F_{19}, A_{21}, and D_{23} shown. (b) Dimer subunit of the tetramer with the side chains of L_{17}, F_{19}, A_{21}, D_{23}, I_8, and I_{11} shown.

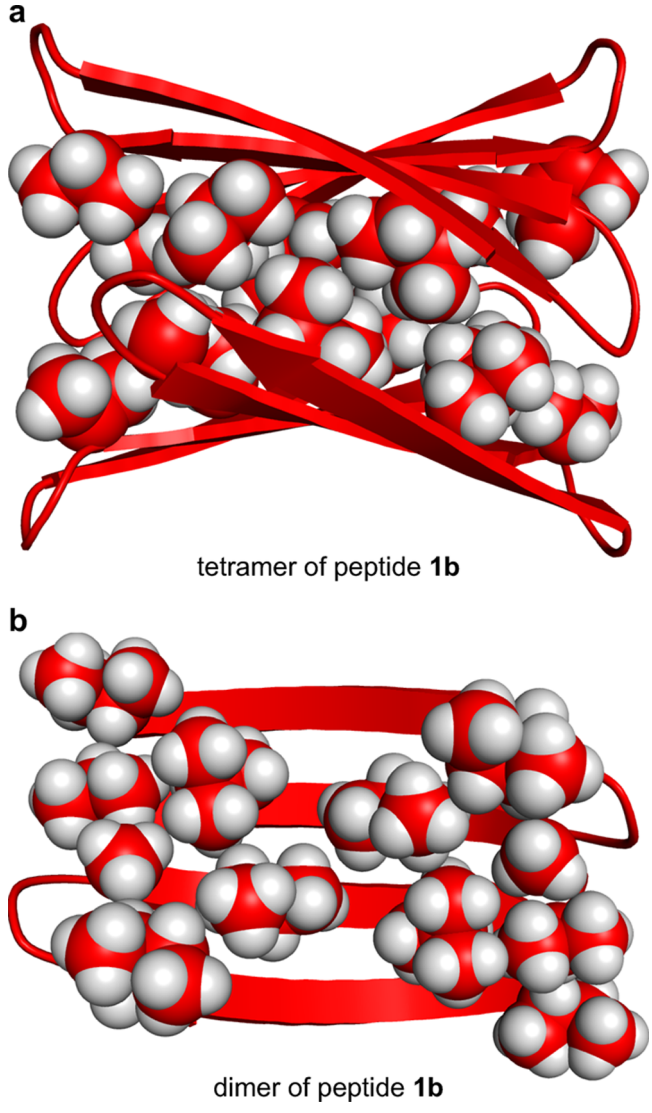

Figure 11. Molecular model of the tetramer formed by peptide **1b**. (a) The tetramer with the side chains of A_{30}, I_{32}, L_{34}, and V_{36} shown. (b) Dimer subunit of the tetramer with the side chains of A_{30}, I_{32}, L_{34}, V_{36}, I_8, and I_{11} shown.

and D_{23} are exposed to solvent. The β-sheet dimers do not completely overlap, but rather are rotated roughly 30° about the normal axis. The rotation and twist of the β-sheets allow the corners to pack tightly against each other. The corners of the β-sheet layers are nearly in contact, which is consistent with the observed interlayer NOEs between the Hao protons and the I_{11} side-chain protons.

The energy-minimized model of the peptide **1b** tetramer is similar to that of peptide **1a** in that it also consists two four-stranded β-sheets that laminate together (Figure 11). The β-sheets are slightly less twisted, and the side chains of A_{30}, I_{32}, L_{34}, and V_{36} form the hydrophobic surface that packs in the hydrophobic core. Like peptide **1a**, the β-sheets are rotated roughly 30° about the normal axis, allowing the corners to pack tightly against each other.

CONCLUSION

Macrocyclic β-sheet peptides **1** provide a platform with which to study the self-assembly of amyloid-derived peptides. Essential to the design of these β-sheet-forming peptides is the use of an amphiphilic template strand containing the peptide sequence IKHaoKI to block uncontrolled aggregation. The unnatural amino acid Hao promotes β-sheet formation and blocks uncontrolled hydrogen-bonding interactions. The Ile residues in the template strand give a distinct hydrophobic surface that promotes peptide assembly, while the Lys residues give a distinct hydrophilic surface that disfavors aggregation.

Incorporation of the central and C-terminal regions of Aβ into peptides **1** allows the study of these regions. The peptides containing these regions assemble through hydrogen-bonding and hydrophobic interactions to form β-sheet dimers that further assemble to form tetramers. NOESY and other ^{1}H NMR studies show that the tetramers comprise a β-sandwich of two hydrogen-bonded dimers. Molecular modeling further elucidates the structures of the tetramers. The tetramers that form reflect the propensities of the central and C-terminal regions to assemble and adopt β-sheet structure.

Incorporation of a single ^{15}N isotopic label into peptides **1** provides a spectroscopic probe that simplifies the spectra of the monomers and tetramers. ^{1}H,^{15}N HSQC studies show that

DOI: 10.1021/jacs.6b06000
J. Am. Chem. Soc. 2016, 138, 13882−13890

each peptide gives a single crosspeak associated with the monomer and a single crosspeak associated with the tetramer. ^{15}N-Edited NOESY studies corroborate the pairing of the dimers within the tetramers. The hydrophobic amino acids Gly, Ala, Val, Leu, Ile, and Phe are widespread in amyloidogenic peptides and proteins and are readily available with an ^{15}N isotopic label at reasonable cost. The incorporation of a single ^{15}N-labeled amino acid as a spectroscopic probe promises to be broadly useful in studying the assembly and coassembly of peptides. In the accompanying paper, we apply this approach to study the coassembly of peptides derived from the central and C-terminal regions of Aβ.

■ ASSOCIATED CONTENT

Supporting Information

The Supporting Information is available free of charge on the ACS Publications website at DOI: 10.1021/jacs.6b06000.

Figures S1−S8, showing ^{1}H NMR and NOESY spectra and key NOEs; procedures for the synthesis of peptides **1** and also for the Fmoc-protection of ^{15}N-labeled amino acids; HPLC and MS characterization data for peptides **1**; and NMR spectroscopic data for peptides **1**, [^{15}N]**1**, Fmoc-[^{15}N]Phe-OH, and Fmoc-[^{15}N]Gly-OH (PDF)

■ AUTHOR INFORMATION

Corresponding Author

*jsnowick@uci.edu

Notes

The authors declare no competing financial interest.

■ ACKNOWLEDGMENTS

We thank the National Institutes of Health for grant support (GM097562). N.L.T. thanks Prof. Melanie J. Cocco and Dr. Philip R. Dennison for assistance with the NMR experiments.

■ REFERENCES

(1) (a) Selkoe, D. J. *Nature* **2003**, *426*, 900−904. (b) Ross, C. A.; Poirier, M. A. *Nat. Med.* **2004**, *10*, S10−S17. (c) Chiti, F.; Dobson, C. M. *Annu. Rev. Biochem.* **2006**, *75*, 333−366. (d) Knowles, T. P.; Vendruscolo, M.; Dobson, C. M. *Nat. Rev. Mol. Cell Biol.* **2014**, *15*, 384−396.

(2) (a) Näslund, J.; Haroutunian, V.; Mohs, R.; Davis, K. L.; Davies, P.; Greengard, P.; Buxbaum, J. D. *JAMA* **2000**, *283*, 1571−1577. (b) Haass, C.; Selkoe, D. J. *Nat. Rev. Mol. Cell Biol.* **2007**, *8*, 101−112. (c) Querfurth, H. W.; LaFerla, F. M. *N. Engl. J. Med.* **2010**, *362*, 329−344.

(3) Kirkitadze, M. D.; Bitan, G.; Teplow, D. B. *J. Neurosci. Res.* **2002**, *69* (5), 567−77.

(4) (a) Petkova, A. T.; Ishii, Y.; Balbach, J. J.; Antzutkin, O. N.; Leapman, R. D.; Delaglio, F.; Tycko, R. *Proc. Natl. Acad. Sci. U. S. A.* **2002**, *99*, 16742−16747. (b) Paravastu, A. K.; Leapman, R. D.; Yau, W.-M.; Tycko, R. *Proc. Natl. Acad. Sci. U. S. A.* **2008**, *105*, 18349−18354. (c) Tycko, R.; Wickner, R. B. *Acc. Chem. Res.* **2013**, *46*, 1487−1496. (d) Lu, J.-X.; Qiang, W.; Yau, W.-M.; Schwieters, C. D.; Meredith, S. C.; Tycko, R. *Cell* **2013**, *154*, 1257−1268.

(5) The fibrils formed by Aβ_{1-42} adopt a more compact structure: (a) Xiao, Y.; Ma, B.; McElheny, D.; Parthasarathy, S.; Long, F.; Hoshi, M.; Nussinov, R.; Ishii, Y. *Nat. Struct. Mol. Biol.* **2015**, *22*, 499−505. (b) Walti, M. A.; Ravotti, F.; Arai, H.; Glabe, C. G.; Wall, J. S.; Bockmann, A.; Guntert, P.; Meier, B. H.; Riek, R. *Proc. Natl. Acad. Sci. U. S. A.* **2016**, *113*, E4976−E4984. (c) Colvin, M. T.; Silvers, R.; Ni, Q. Z.; Can, T. V.; Sergeyev, I.; Rosay, M.; Donovan, K. J.; Michael, B.; Wall, J.; Linse, S.; Griffin, R. G. *J. Am. Chem. Soc.* **2016**, *138*, 9663−9674.

(6) (a) Cleary, J. P.; Walsh, D. M.; Hofmeister, J. J.; Shankar, G. M.; Kuskowski, M. A.; Selkoe, D. J.; Ashe, K. H. *Nat. Neurosci.* **2005**, *8*, 79−84. (b) Benilova, I.; Karran, E.; De Strooper, B. *Nat. Neurosci.* **2012**, *15*, 349−357. (c) Teplow, D. B. *Alzheimer's Res. Ther.* **2013**, *5*, 39−51. (d) Walsh, D. M.; Selkoe, D. J. *J. Neurochem.* **2007**, *101*, 1172−1184.

(7) Liu, R.; McAllister, C.; Lyubchenko, Y.; Sierks, M. R. *J. Neurosci. Res.* **2004**, *75*, 162−171.

(8) (a) Esler, W. P.; Stimson, E. R.; Ghilardi, J. R.; Lu, Y. A.; Felix, A. M.; Vinters, H. V.; Mantyh, P. W.; Lee, J. P.; Maggio, J. E. *Biochemistry* **1996**, *35*, 13914−13921. (b) Cukalevski, R.; Boland, B.; Frohm, B.; Thulin, E.; Walsh, D.; Linse, S. *ACS Chem. Neurosci.* **2012**, *3*, 1008−1016. (c) Tjernberg, L. O.; Callaway, D. J. E.; Tjernberg, A.; Hahne, S.; Lilliehook, C.; Terenius, L.; Thyberg, J.; Nordstedt, C. *J. Biol. Chem.* **1999**, *274*, 12619−12625.

(9) (a) Larini, L.; Shea, J. E. *Biophys. J.* **2012**, *103*, 576−586. (b) Ball, K. A.; Phillips, A. H.; Wemmer, D. E.; Head-Gordon, T. *Biophys. J.* **2013**, *104*, 2714−2724. (c) Do, T. D.; LaPointe, N. E.; Nelson, R.; Krotee, P.; Hayden, E. Y.; Ulrich, B.; Quan, S.; Feinstein, S. C.; Teplow, D. B.; Eisenberg, D.; Shea, J. E.; Bowers, M. T. *J. Am. Chem. Soc.* **2016**, *138*, 549−557.

(10) (a) Hoyer, W.; Gronwall, C.; Jonsson, A.; Stahl, S.; Hard, T. *Proc. Natl. Acad. Sci. U. S. A.* **2008**, *105*, 5099−5104. (b) Cerf, E.; Sarroukh, R.; Tamamizu-Kato, S.; Breydo, L.; Derclaye, S.; Dufrene, Y. F.; Narayanaswami, V.; Goormaghtigh, E.; Ruysschaert, J. M.; Raussens, V. *Biochem. J.* **2009**, *421*, 415−423. (c) Yu, L.; Edalji, R.; Harlan, J. E.; Holzman, T. F.; Lopez, A. P.; Labkovsky, B.; Hillen, H.; Barghorn, S.; Ebert, U.; Richardson, P. L.; Miesbauer, L.; Solomon, L.; Bartley, D.; Walter, K.; Johnson, R. W.; Hajduk, P. J.; Olejniczak, E. T. *Biochemistry* **2009**, *48*, 1870−1877. (d) Sandberg, A.; Luheshi, L. M.; Söllvander, S.; Pereira de Barros, T.; Macao, B.; Knowles, T. P. J.; Biverstål, H.; Lendel, C.; Ekholm-Petterson, F.; Dubnovitsky, A.; Lannfelt, L.; Dobson, C. M.; Härd, T. *Proc. Natl. Acad. Sci. U. S. A.* **2010**, *107*, 15595−15600. (e) Lendel, C.; Bjerring, M.; Dubnovitsky, A.; Kelly, R. T.; Filippov, A.; Antzutkin, O. N.; Nielsen, N. C.; Hard, T. *Angew. Chem., Int. Ed.* **2014**, *53*, 12756−12760. (f) Spencer, R. K.; Li, H.; Nowick, J. S. *J. Am. Chem. Soc.* **2014**, *136*, 5595−5598. (g) Kreutzer, A. G.; Hamza, I. L.; Spencer, R. K.; Nowick, J. S. *J. Am. Chem. Soc.* **2016**, *138*, 4634−4642.

(11) (a) Cheng, P. N.; Liu, C.; Zhao, M.; Eisenberg, D.; Nowick, J. S. *Nat. Chem.* **2012**, *4*, 927−933. (b) Liu, C.; Zhao, M.; Jiang, L.; Cheng, P. N.; Park, J.; Sawaya, M. R.; Pensalfini, A.; Gou, D.; Berk, A. J.; Glabe, C. G.; Nowick, J.; Eisenberg, D. *Proc. Natl. Acad. Sci. U. S. A.* **2012**, *109*, 20913−20918. (c) Buchanan, L. E.; Dunkelberger, E. B.; Tran, H. Q.; Cheng, P. N.; Chiu, C. C.; Cao, P.; Raleigh, D. P.; de Pablo, J. J.; Nowick, J. S.; Zanni, M. T. *Proc. Natl. Acad. Sci. U. S. A.* **2013**, *110*, 19285−19290.

(12) Nowick, J. S.; Chung, D. M.; Maitra, K.; Maitra, S.; Stigers, K. D.; Sun, Y. *J. Am. Chem. Soc.* **2000**, *122*, 7654−7661.

(13) (a) Nowick, J. S.; Brower, J. O. *J. Am. Chem. Soc.* **2003**, *125*, 876−877. (b) Woods, R. J.; Brower, J. O.; Castellanos, E.; Hashemzadeh, M.; Khakshoor, O.; Russu, W. A.; Nowick, J. S. *J. Am. Chem. Soc.* **2007**, *129*, 2548−2558.

(14) For some related studies of peptide and protein coassembly, see: (a) Hammarstrom, P.; Schneider, F.; Kelly, J. W. *Science* **2001**, *293*, 2459−2462. (b) Schnarr, N. A.; Kennan, A. J. *J. Am. Chem. Soc.* **2002**, *124*, 9779−9783. (c) Hadley, E. B.; Testa, O. D.; Woolfson, D. N.; Gellman, S. H. *Proc. Natl. Acad. Sci. U. S. A.* **2008**, *105*, 530−535. (d) Xu, F.; Zahid, S.; Silva, T.; Nanda, V. *J. Am. Chem. Soc.* **2011**, *133*, 15260−15263. (e) Fallas, J. A.; Hartgerink, J. D. *Nat. Commun.* **2012**, *3*, 1087. (f) Thomas, F.; Boyle, A. L.; Burton, A. J.; Woolfson, D. N. *J. Am. Chem. Soc.* **2013**, *135*, 5161−5166. (g) Negron, C.; Keating, A. E. *J. Am. Chem. Soc.* **2014**, *136*, 16544−16556.

(15) Truex, N. L.; Nowick, J. S. *J. Am. Chem. Soc.* **2016**, DOI: 10.1021/jacs.6b06001.

(16) ^{1}H NMR studies were performed without buffer at pH 2.5 ± 0.5 to keep peptides **1a** and **1b** in the fully protonated state.

(17) (a) Khakshoor, O.; Demeler, B.; Nowick, J. S. *J. Am. Chem. Soc.* **2007**, *129*, 5558−5569. (b) Pham, J. D.; Demeler, B.; Nowick, J. S. *J.*

Am. Chem. Soc. **2014**, *136*, 5432−5442. (c) Pham, J. D.; Spencer, R. K.; Chen, K. H.; Nowick, J. S. *J. Am. Chem. Soc.* **2014**, *136*, 12682−12690.

(18) (a) Polson, A. *J. Phys. Colloid Chem.* **1950**, *54*, 649−652. (b) Teller, D. C.; Swanson, E.; de Haën, C. *Methods Enzymol.* **1979**, *61*, 104−124. (c) Yao, S.; Howlett, G. J.; Norton, R. S. *J. Biomol. NMR* **2000**, *16*, 109−119. (d) Cohen, Y.; Avram, L.; Frish, L. *Angew. Chem., Int. Ed.* **2005**, *44*, 520−554. (e) Cohen, Y.; Avram, L.; Evan-Salem, T.; Slovak, S.; Shemesh, N.; Frish, L. In *Analytical Methods in Supramolecular Chemistry*, 2nd ed.; Schalley, C. A., Ed.; Wiley-VCH: Weinheim, 2012; pp 197−285.

(19) The ratio of diffusion coefficients of an oligomer and monomer reflects the oligomerization state as well as the shapes of the molecules. A tetramer will have a diffusion coefficient of about 0.59−0.63 times that of the monomer, while a dimer will have a diffusion coefficient of about 0.75−0.79 times that of the monomer. A tetramer could not easily be distinguished from a pentamer and could only marginally be distinguished from a trimer on the basis of diffusion coefficients measured by DOSY. The observation of well-defined dimer subunits by NOESY in conjunction with the observed ratios of diffusion coefficients by DOSY clearly establishes the tetrameric state of the oligomers.

(20) Chemical exchange between the monomer and tetramer of peptide **1a** is slow on the hundred-millisecond time scale at 298 K, but exchange increases at higher temperatures. An EXSY experiment shows a set of EXSY crosspeaks that indicate chemical exchange on the hundred-millisecond time scale at 318 K (see the Supporting Information). In contrast, chemical exchange between the monomer and tetramer of peptide **1b** occurs on the hundred-millisecond time scale even at 293 K.

DOI: 10.1021/jacs.6b06000
J. Am. Chem. Soc. 2016, 138, 13882−13890